

An Investigation on the Effects of Optimum Forming Parameters in Hydro-mechanical Deep Drawing Process Using the Genetic Algorithm

Saeed Yaghoubi^a, Faramarz Freseshteh-Saniee^{a, *}

^a Department of Mechanical Engineering, Faculty of Engineering, Bu-Ali Sina University, Hamedan, Iran

ARTICLE INFO

Article history:

Received: 02 December 2017

Accepted: 20 January 2018

Keywords:

Hydro-mechanical Deep Drawing
Maximum Reduction in Sheet Thickness
Product Uniformity
Neural Network
Genetic Algorithm

ABSTRACT

The present research work is concerned with the effects of optimum process variables in elevated temperature hydro-mechanical deep drawing of 5052 aluminum alloy. Punch-workpiece and die-workpiece friction coefficients together with the initial gap between the blank holder and matrix were considered as the process variables which, in optimization terminology, are called design parameters. Since both the maximum reduction in sheet thickness and the final product uniformity (thickness variation) are important in the hydro-mechanical deep drawing, they are selected as the objective functions for optimization. After conducting 27 finite-element simulations of the operation and validation of the numerical results, a neural network was trained and combined with the genetic algorithm to obtain the optimum design parameters. The outcomes of this investigation have shown that these optimized process variables simultaneously resulted in the best values for both the objective functions, in comparison with all the conducted finite-element analyses.

1. Introduction

Production methods and their development have been of very important areas in different periods of human life. Among various production methods, metal forming processes have been specifically important, which can be attributed to the production of parts with excellent mechanical properties, least material loss, and extensive application in manufacturing industries, such as automotive industry and machinery industries. The main objective in a metal forming process is optimal forming of raw materials (with relatively simple geometries) into a product with relatively complex shape through one or more forming operations. Metal sheets are among the most common industrial raw materials. Hydroforming, as a metal forming method, is indeed a deep drawing process that uses a high pressure hydraulic fluid. Due to its many advantages, it is superior over ordinary deep drawing processes. The sheet metal hydroforming process is similar to the traditional deep drawing process, through which the initial sheet metal is held by a blank holder and drawn into a die by a punch [1]. The major difference between the sheet hydroforming and traditional deep drawing processes is the use of a fluid, in addition to the punch, in the former one. Forming complex parts, higher dimensional accuracy due to spring-back reduction, desirable surface roughness and no need for a complex

die, highly desirable uniform thickness, drawing of complex parts in a single stage, and greater deep drawing along with desirable strain distribution are among advantages of this method over deep drawing process, resulting in reduced costs [2]. The hydroforming process has different types including hydro-mechanical deep drawing with radial pressure. Fig. 1 presents a schematic of this method. The radial pressure on the edge of the blank facilitates the drawing of sheet into the forming die, thereby increasing drawing ratio and reducing forming force [3]. Light alloys, such as aluminum and magnesium, are good substitutes for steel in different industries, specifically in aerospace and automotive industries. This is due to their high strength/weight ratios and high corrosion resistance (as one of aluminum properties). The main disadvantages of these alloys are their low toughness and formability at the room temperature. The hydroforming process at elevated temperatures has been introduced to eliminate this problem and reduce the yield strength of the sheet, thereby decreasing the forming force [4]. Temperature is among the most important factors in metal forming. The application of elevated temperature in forming process increases limit drawing ratio (LDR) and improves the thickness distribution [5]. Although studies into hydroforming process at the elevated temperatures have been initiated since 1997, practical difficulties have prevented the conduction of

* Corresponding author: Yaghoubisaeed@gmail.com

extensive research [6]. Choi et al. investigated the hydroforming mechanism at the elevated temperature for a light alloy sheet [7]. It was observed that the flange temperature should be remained high in the hot deep drawing of aluminum alloys to facilitate the material flow. In contrast, the punch temperature should be kept low to increase the drawability. Hosseinpoor et al. investigated the application of hydrodynamic deep drawing with a radial pressure on aluminum alloy 5052 at elevated temperatures [8]. In their experiments, they used heat transfer oil with viscosity of 100 CST, which could resist up to 300°C. The experiments were conducted at 200°C, maximum pressure of 32 MPa, and punch speed of 50, 150, and 200 mm/min. Results showed that the forming force of the punch initially increased and then decreased. This was due to the flow of material on the punch tip and die entrance radius after initial contact between the punch and the sheet. After the early stage of forming operation, the work hardening phenomenon enhanced the resistance to greater deformation. Gedikli et al. investigated the reduction in sheet thickness and cavity filling ratio (CFR) of aluminum at different strain rates and elevated temperatures through conducting experiments and simulations [9]. Their findings revealed that sheet thickness decreased and filling rate increased with increasing the temperature. Finally, the explicit and implicit problem solving methods were compared and showed that the former one produced a more accurate estimation for the simulated model. Hashemi et al. [10] investigated the application of hydrodynamic deep drawing with radial pressure on 1050 aluminum alloy and pure copper. The path of the fluid pressure, sheet property, and its thickness were among parameters considered by them. Their findings showed that sheets with lower initial thickness and greater strength were more formable and had less thickness reduction. Desu et al. [11] compared deep drawing and hydrodynamic deep drawing processes at elevated temperatures through some experiments and comparison with simulation results. Parameters investigated in their study were limit drawing ratio, von Mises stress, and thickness distribution in the final product. The maximum punch force was another parameter investigated by them. This force was greater in the hydrodynamic deep drawing process than that of the traditional deep drawing one. The parameters affecting this force were the clearance between the punch and die, and maximum pressure in the forming die.

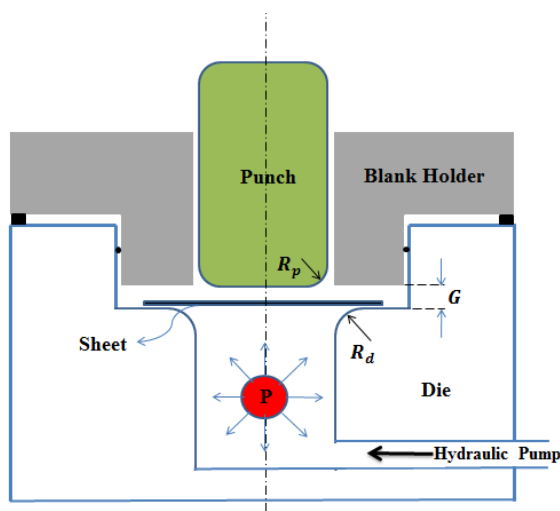


Figure 1. Schematic of hydro-mechanical deep drawing process.

The punch force in the sheet forming process is less important than in the bulk forming process. This is because of lower

magnitude of the punch force in the former operation. Instead, in many relevant studies, the maximum reduction in sheet thickness has been regarded as the objective function. In addition to the maximum reduction in sheet thickness, uniformity and surface quality of the final product are also two important parameters in sheet metal forming. There are many factors affecting maximum reduction in sheet thickness and product uniformity, including friction between the punch/matrix and the primary sheet, and the distance between the matrix and blank holder (Figure 1). In this study, the hydro-mechanical deep drawing process at elevated temperatures for aluminum sheet was first simulated and validated through comparison with experimental results existing in the literature. Furthermore, a neural network was trained to investigate the behavior of this operation for different values of the process variables. Finally, the optimal results of the design parameters were introduced to minimize the maximum reduction in thickness and enhance product uniformity.

2. Properties of Materials

The material used in this study was aluminum alloy 5052. Fig.2 presents its true stress-strain curves for various temperatures and strain rates. According to this figure, the yield stress decreases and maximum elongation increases with increasing temperature and decreasing the rate of strain. This was because of strength reduction and material flow improvement.

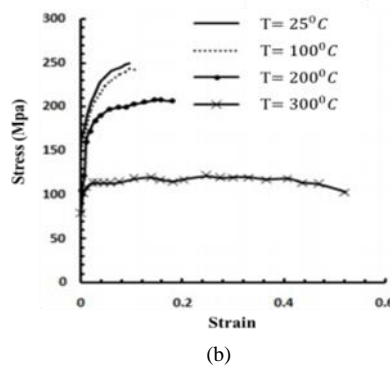
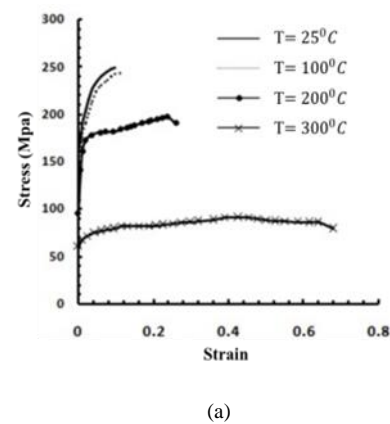


Figure 2. True stress-strain curve of aluminum alloy 5052 (a) strain rate (s^{-1}) of 0.0013, (b) strain rate (s^{-1}) of 0.013 [12].

3. Finite Element Simulations

In the present research work, ABAQUS was used to numerically simulate the hydro-mechanical deep drawing process

at elevated temperatures. Knowing that the die set and process were symmetric, to reduce the solution time, an axially symmetric model was employed and one-fourth of the whole set was modeled. Deformable sheet was modeled using four-node axisymmetric elements (CAX4RT). As the name of this element conveys, in addition to displacement, it has a single free degree of freedom of temperature. The punch, blank holder, and matrix were modeled as analytical rigid parts. Fig. 3 illustrates the position of elements of this process in the beginning of the numerical simulation.

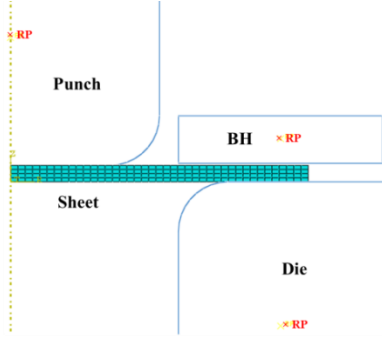


Figure 3. Finite element model of hydro-mechanical deep drawing operation created in ABAQUS.

The initial geometrical parameters of the simulation process are summarized in Table 1. Mechanical properties of the given aluminum sheet are also presented in Table 2 [12]. To define behavior of the material in ABAQUS, data of stress-strain curves (Fig. 2) were introduced to the software as data tables for two strain rates of $0.0013 \text{ (s}^{-1}\text{)}$ and $0.013 \text{ (s}^{-1}\text{)}$. In the interaction module, a contact surface was defined between the sheet and other elements. In addition, the coefficients of friction between the sheet and the punch and sheet with the blank holder were selected to be 0.15 and 0.06, respectively [8].

Table 1. Geometrical parameters of the die set.

Parameter	Value (mm)
Initial Sheet Diameter	72
Initial Sheet Thickness	2
Inner Diameter of the Matrix	40.60
Punch Diameter	36
The Corner Radius of Both the Punch and Matrix	6
Clearance Between Sheet and Blank Holder	0.25

Table 2. Mechanical and physical properties of 5052 aluminum alloy [12].

Properties	Value
Yield Stress (MPa)	89.60
Density ($\frac{Kg}{m^3}$)	2680
Young's Modulus (GPa)	70.30
Poisson's Ratio	0.33

The coefficient of friction between various surfaces was considered to be constant [13]. The numerical simulation was conducted in a single stage as a coupled temperature-displacement process. Process modeling was done through dynamic explicit solution, based on the research conducted by Gedikli et al. [9]. After the introduction of displacement and temperature boundary conditions, a uniform pressure distribution of the fluid (radial pressure) was defined equal to 32 MPa in the underlying and lateral of the sheet surfaces [8].

4. Neural Network and Optimization

In this section, mechanism of neural network training was explained and then the genetic optimization algorithm is introduced.

4.1. Training Neural Network

Humans have always looked to nature and living systems for inspiration to solve different problems, resulting in valuable achievements. Initial attempts to model human brain and neural network have led to the development of a model that presents the process function of a unit of the brain, namely neuron. An artificial neural network is a combination of some units, named neurons. The input of this neuron is multiplied by the weights and then is added to a constant number, namely bias. The result is introduced to a non-linear function to produce the output [14]. Fig. 4 presents the schematic of this process. The number of neurons per hidden layer of a neural network has a significant effect on its performance.

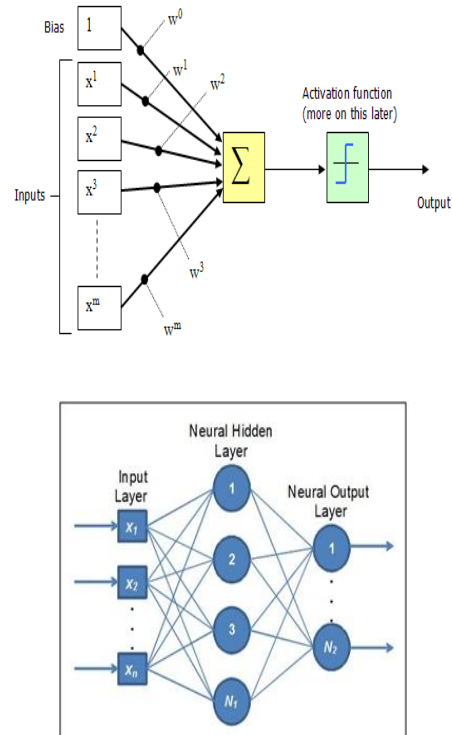


Figure 4. Structure of artificial neural network, along with a neuron model [15].

Selection of the number of neurons is in fact a compromise between convergence and the ability to generalize the network.

Multilayer neural networks are able to perform a non-linear mapping with desirable accuracy through an appropriate selection of the number of layers and neural cells, which are usually not much. Three inputs and two outputs were considered in this study. Therefore, the artificial neural network should be trained by data once again. The first neural network was trained with the first three inputs and outputs, and the second neural network with the second inputs and outputs. To make a relationship between the inputs and outputs of the numerical experiments and develop an appropriate estimation function, a network with a hidden layer containing 10 neurons, tangent-sigmoid transfer function, an output layer with 24 neurons, and a transfer function were trained linearly. A schematic of this network is presented in Fig. 5. The network was trained with the Levenberg-Marquardt algorithm. In this network, 17 data units were randomly selected by the software to train the neural network, 5 data to test the network, and 5 data to validate it during the training.

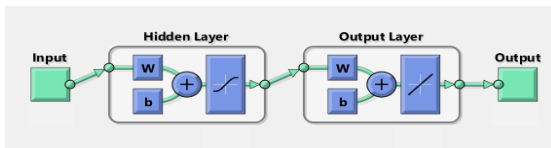


Figure 5. Neural network designed for simulation results.

4.2. Genetic Algorithm

The genetic algorithm is inspired by the nature based on 'survival-of-the-fittest' law of Darwin's Evolution Theory. The genetic algorithm was developed by John Holland, a computer specialist at the University of Michigan, in 1962. He introduced the main concepts of genetic algorithm (i.e. selection, crossover, and mutation operators used in artificial networks) in an article, entitled "Adaptation in Natural and Artificial Systems." He also addressed the mathematical basis of the genetic algorithm. In this method, chromosomes with high fitness had more chance to be selected for reproduction in the population selected by the selection process. After the completion of selection process, the operator was applied to the selected direction to produce offspring. In the combination process, a random number is generated for each chromosome by selecting a constant combination rate. If the generated random number is less than the combination rate, the chromosome is selected to crossover with next eligible chromosomes. Then, the mutation operator is applied. The aim is to cause greater dispersion in the range of design space exploration. Finally, genetic algorithm ends when some terms, such as the generation of certain number of population and/or mean standard deviation of individual's performance in a population, are met [16]. Figure 6 presents the solution flowchart of the genetic algorithm.

4.3. Multi-objective Optimization Algorithm

In this investigation, a multi-objective optimization method has been employed to specify dominating peripheral parameters of the hydrodynamic deep drawing, using the evolutionary genetic algorithm and objective functions i.e. maximum reduction of sheet thickness and enhancing the quality (uniformity) of the final product. In a multi-objective optimization method, different objective functions may be defined and minimized. These objective functions should interact such that the improvement of one of them should lead to enhancement of the other. Therefore, such problems are not

limited to one solution, rather a set of optimal solutions, called optimal Pareto or Pareto front, are defined for multi-objective optimizations. Pareto front in objective functions and optimization problems refers to a set of solutions with no superiority over each other; however, they produce better solutions for objective functions in the search space [17]. Therefore, a new population is generated from an initial population and ranked. Then, the Pareto front is updated and the final Pareto front is achieved by calculating fitness values based on the ranked results and the application of appropriate termination criterion. Mathematically, the optimization problem generally refers to finding of the vector $X^* = [x_1^*, x_2^*, \dots, x_n^*]^T$ for optimization of the function according to the following Equation [18].

$$F(X) = [f_1(X), f_2(X), \dots, f_k(X)]^T \quad (1)$$

It includes m inequality constraints and p equality constraints as Equations 2 and 3, respectively.

$$g_i(X) \leq 0, i = 1:m \quad (2)$$

$$h_j(X) = 0, j = 1:p \quad (3)$$

In Equation 1, X is the vector of input variables and $F(X)$ is the vector of objective functions, which should be minimized.

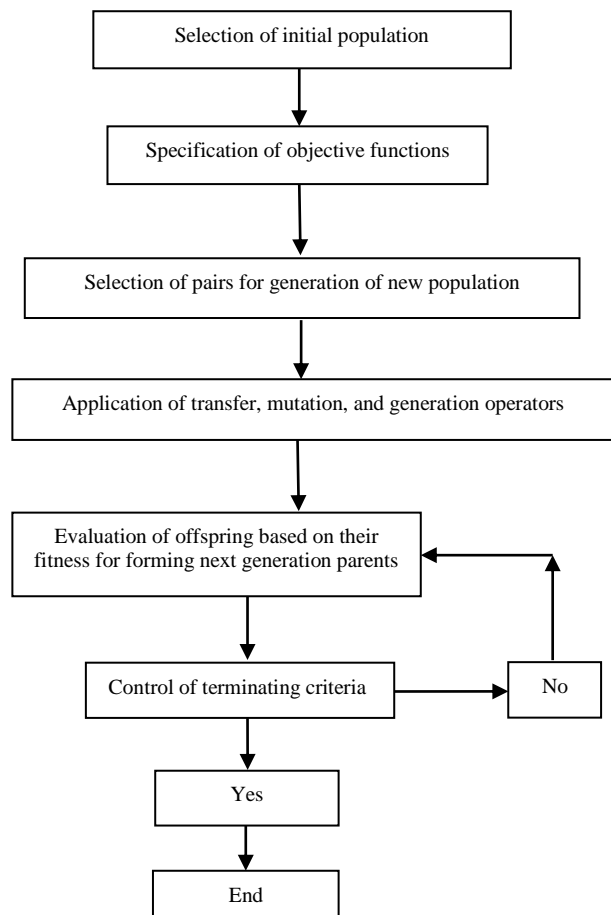


Figure 6. Genetic algorithm flowchart [18].

5. Results and Discussion

Fig. 7 shows the punch and the deformed sheet. The percentage reduction in sheet thickness is a parameter used for examining the quality of the final product. Equation 4 was used to calculate the percentage reduction in sheet thickness [19].

$$R_{th} = \frac{t_0 - t_f}{t_0} \times 100 \quad (4)$$

where, t_0 and t_f are respectively the initial and final thicknesses of the sheet. According to Fig. 7, the maximum reduction in thickness of the deformed sheet occurred where the punch edge contacted the sheet (presented by a circle).

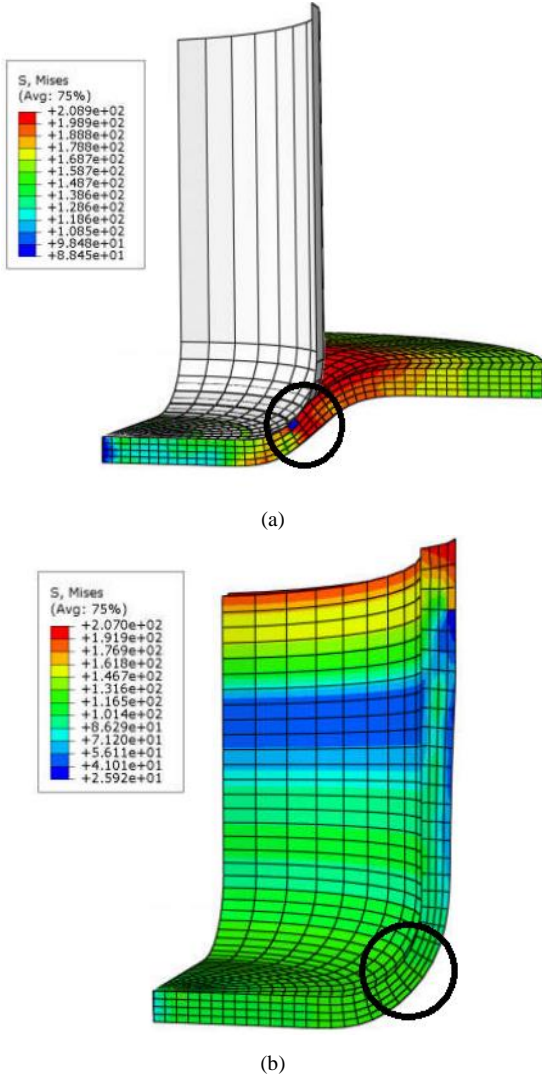


Figure 7. Schematic of a deformed sheet (a) early stage of sheet deformation, (b) final sheet product.

Regarding the punch geometry and its contact with the sheet, this deformation is acceptable. To validate the simulation results, the thickness distribution diagram, based on the distance from the workpiece center, is compared with the experimental one obtained from [8] (Fig. 8). According to diagrams shown in Fig. 8, the trend and magnitude of thickness distribution in the simulation are acceptably consistent with the experimental results. The greatest point-to-point thickness difference between the simulation and experimental finding was found to 6.25%. in addition, the total difference between all points in these two

diagrams was 26.10%. Figure 8 confirms the accuracy of the obtained numerical results. Moreover, diagrams in this figure suggest that the maximum reduction in sheet thickness has occurred where the punch contacted the sheet (Fig. 7).

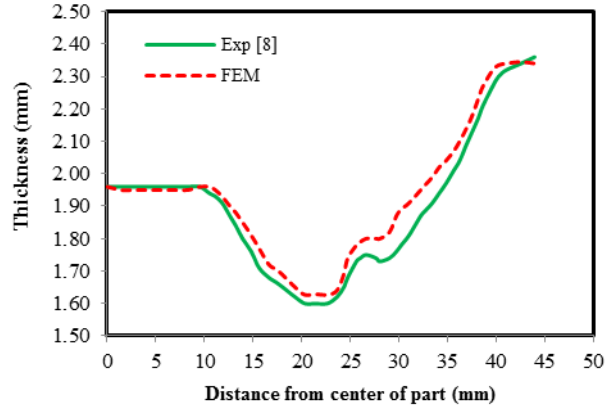


Figure 8. A comparative diagram of the thickness distribution based on the distance from the center of workpiece.

The final product of a sheet forming process should have desirable quality. Many factors can be regarded as a quality indicator of the final product, including greater uniformity and lower reduction in sheet thickness. Greater uniformity means that the thickness of the deformed sheet in different areas of the final product has the least difference with the mean sheet thickness. In other words, the lower the difference between the final product thickness and the mean sheet thickness, the lower become the thickness variation and the greater is the uniformity. With this regard, equation 5 was used to calculate the percentage of thickness variation.

$$V_{th} = \sum_{i=1}^n \left| \frac{t_{ave} - t_i}{t_{ave}} \right| \quad (5)$$

where n is the number of points on the thickness distribution curve based on the distance from the workpiece center, t_{ave} is the mean thickness of the deformed sheet, and t_i is the sheet thickness at each point. It is worth noting that both the thickness variation and percentage of thickness reduction are dimensionless. Since some parameters have a greater impact on the product uniformity and some others on the maximum reduction in thickness, the current study has considered both the parameters as the objective functions in optimization. Reduction of thickness variation of the final product relative to the initial sheet in all the points on the diagram (enhanced quality of the final product) and also decreasing maximum reduction in the sheet thickness were both desirable and, therefore, the aim was to find the minimum value of these two functions.

Many factors, including the friction coefficient and clearance, affect the maximum reduction in sheet thickness and thickness variation of the final product. The desirable parameters in this study were considered to be the coefficient of friction between the punch and the sheet (Fr_{Sh-P}), coefficient of friction between the matrix and the sheet (Fr_{Sh-D}), and the gap between the sheet and the blank holder (G). Values of these parameters can also affect other variables. It should be noted that the selected ranges for these parameters were considered based on previous studies [8-11].

- Coefficient of friction between the punch and the sheet:** It is a contact parameter that affects the sheet forming. Fig. 9 presents the effect of an increase in friction between the punch and the sheet on reduction in thickness and thickness variation of the final product. The contact between the punch and sheet increases with increasing the friction coefficient. In addition, thickness variation decreases and product uniformity improves with preventing the slipping of the sheet where the punch contacts it.

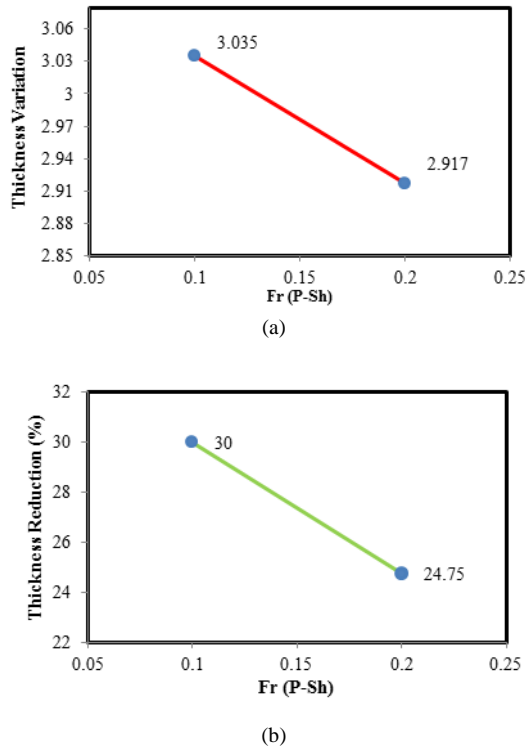


Figure 9. Effect of an increase in friction between punch and sheet on (a) thickness variation of the final product and (b) maximum reduction in thickness.

- Coefficient of friction between the matrix and the sheet:** It is another factor affecting the product uniformity and maximum reduction in thickness. Fig. 10 illustrates a diagram showing the effect of reduction in thickness and thickness variation of the final product by a change in friction between the sheet and the matrix. Since the contact (thereby friction) between the matrix and sheet increases in the flange area with increasing the friction coefficient, a greater thickness reduction is expected, where the punch contacts the sheet; in addition, lower product uniformity is obtained.
- Distance between Matrix and Blank Holder:** It is also an important factor affecting sheet forming in a hydro-mechanical deep drawing process. The effects of changes in this factor on reduction in thickness and thickness variation of the final product are presented in Fig. 11. With increasing the distance between the matrix and the blank holder, the sheet edge wrinkling occurs, resulting in a negative impact on the product uniformity. Values shown in Fig. 11 confirm this phenomenon.

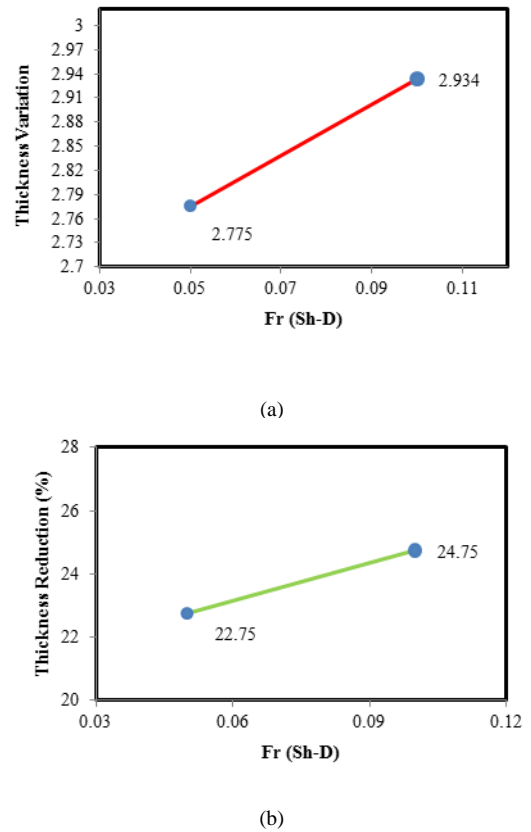


Figure 10. (a) Thickness variation of the final product and (b) maximum reduction in thickness by changing the coefficient of friction between the matrix and the sheet.

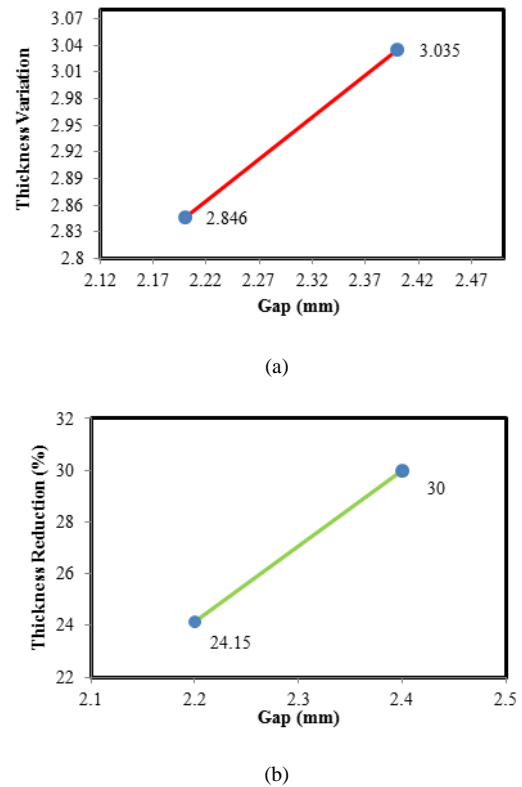


Figure 11. The effect of the gap between the blank holder and matrix on (a) thickness variation of the product and (b) maximum reduction in sheet thickness.

5.1. Designing Numerical Experiments

The forming parameters that affect the final product in this study are the coefficient of friction between the punch and the sheet (Fr_{Sh-P}), coefficient of friction between the matrix and the sheet (Fr_{Sh-D}), and the distance between the matrix and the blank holder (G). Three values were assigned to each parameter. Table 3 represents the values of objective functions for 27 simulations. Previous studies optimized environmental and geometric parameters of the hydro-mechanical deep drawing process to reduce maximum reduction in sheet thickness and lower the chance of sheet rupture. In addition to the above parameter, uniformity of the final product was also considered in the current study. Values obtained from 27 simulation scenarios, presented in Table 3, indicated the importance of the final product uniformity, along with the maximum reduction in sheet thickness in producing a high quality product. As a result, these two parameters were simultaneously regarded as two objective functions for optimization in this research work. Fig. 12 presents the changes in the objective parameters for different values of the design parameters. According to this figure, the effect of changes in design parameters on both the objective variables is significant. The best and worst results of 27 simulation scenarios were obtained for Experiments 7 and 12, respectively. In test 7 compared with experiment 12, the friction between the punch and sheet was increased, the friction between the matrix and the sheet was decreased, and the distance between the matrix and the blank holder was decreased. Therefore, the decrease in the maximum reduction in thickness and thickness distribution of the final product are examined and confirmed by results obtained from Experiments 7 and 12.

5.2. Optimization Output

MATLAB was used to train the neural network and optimize the obtained results. Fig. 13 presents the Pareto front based diagram for the two given objective functions. The optimized points introduced by the Pareto front are not superior over each other from the perspective of the two given objective functions. Therefore, these points can be introduced as optimal values of the design parameters. Regarding the aim of the current study, i.e. reducing the maximum reduction in thickness (critical thickness increase and improving the final product uniformity and quality (thickness variation reduction), an optimal solution with the greatest minimum thickness and lowest thickness variation was considered. This point is shown with a circle in Figure 13. With this regard, the minimum thickness and thickness variation of the optimal product were 1.65 (equivalent to a maximum reduction in thickness equal to 17.50%) and 2.547, respectively. Values of both objective functions improved as compared to all simulation scenarios. In this point, the values of optimal design parameters for the coefficient of friction between the punch and the sheet, coefficient of friction between the matrix and sheet, and distance between the matrix and blank holder were 0.193, 0.057, and 2.223, respectively. Fig. 14 demonstrates the diagrams of the thickness distribution of the formed sheet in Experiments 7 and 12 (the best and worst simulation scenarios). Moreover, the thickness distribution of the optimal state is compared with the initial thickness of the sheet in this figure.

Table 3. Values obtained for two proposed objective functions in 27 different hydro-mechanical deep drawing simulation scenarios.

Test No.	Fr_{Sh-P}	Fr_{Sh-D}	$G(mm)$	$R_{th}(\%)$	$V_{th}(\%)$
1	0.10	0.050	2.2	23.00	2.801
2	0.10	0.050	2.3	23.45	2.812
3	0.10	0.050	2.4	24.00	2.832
4	0.15	0.050	2.2	22.75	2.775
5	0.15	0.050	2.3	23.35	2.799
6	0.15	0.050	2.4	23.85	2.824
7	0.20	0.050	2.2	22.15	2.751
8	0.20	0.050	2.3	22.50	2.772
9	0.20	0.050	2.4	23.80	2.819
10	0.10	0.075	2.2	24.15	2.846
11	0.10	0.075	2.3	24.60	3.015
12	0.10	0.075	2.4	30.00	3.035
13	0.15	0.075	2.2	23.20	2.843
14	0.15	0.075	2.3	24.20	3.010
15	0.15	0.075	2.4	24.60	3.025
16	0.20	0.075	2.2	23.95	2.837
17	0.20	0.075	2.3	24.10	2.906
18	0.20	0.075	2.4	24.75	2.917
19	0.10	0.100	2.2	25.50	2.966
20	0.10	0.100	2.3	26.25	2.973
21	0.10	0.100	2.4	26.80	3.011
22	0.15	0.100	2.2	24.75	2.934
23	0.15	0.100	2.3	25.60	2.945
24	0.15	0.100	2.4	27.10	2.988
25	0.20	0.100	2.2	24.15	2.943
26	0.20	0.100	2.3	24.55	2.958
27	0.20	0.100	2.4	25.00	2.971

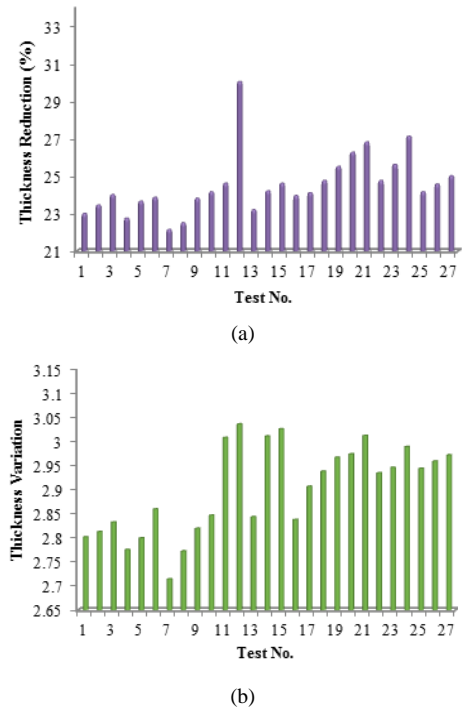


Figure 12. Effect of changes in design parameters on objective parameters (a) maximum reduction in thickness, (b) thickness variation.

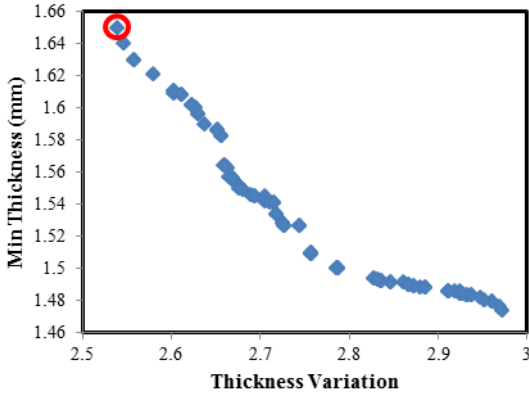


Figure 13. Pareto front of optimal points based on the two objective functions.

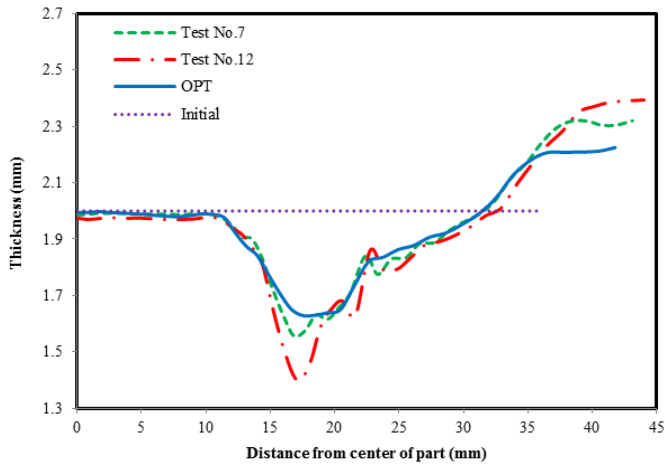


Figure 14. A comparison between the thickness distributions of the optimal, the best, and the worst simulation experiments.

Figure 14 shows the distributions of the reduction in thickness (implying the uniformity improvement), as well as the maximum reduction in thickness of the product. The values in Table 3 indicate that increasing the friction between the punch and sheet, decreasing the friction between the matrix and sheet, and also reducing the distance between the matrix and the blank holder are important in order to produce a high quality product. The optimization results are acceptably consistent with objectives of this investigation. To examine the accuracy of neural network solutions, values of the optimized objective functions obtained from the neural network and genetic algorithm are compared with values of the objective functions obtained from simulation in Table 4. According to this table, the neural network is well trained and has an acceptable error.

Table 4. Comparison of the neural network and FE simulation results for the optimal point.

Objective Function	Simulation	ANN	Error (%)
Maximum Reduction In Thickness (R_{th} %)	17.50	15.93	8.97
Thickness Variation (V_{th})	2.547	2.418	5.06

6. Conclusions

In this study, the hydro-mechanical deep drawing of aluminum alloy 5052 was simulated at an elevated temperature. Forming die parameters are nearly the most important factors affecting the quality of the product. With this regard, the friction between the punch and the sheet, the friction between the matrix and the sheet, and the distance between the blank holder and the matrix were regarded as the input variables. The sheet product should have maximum uniformity (minimum thickness variation) and minimum reduction in thickness. Since, the design variables have different effects on these two parameters; they were regarded as the objective functions in training the neural network and optimization. The main conclusions can be summarized as follows:

- The product uniformity improves with increasing the coefficient of friction between the punch and the sheet. This can be attributed to a greater contact between the sheet and the punch and prevention in sheet slip on the punch.
- Coefficient of friction between the matrix and the sheet was among the parameters affecting hydro-mechanical deep drawing process. Due to a stronger contact between the matrix and the sheet in the flange area with increasing this factor, the produced sample had a greater thickness variation and thus a greater maximum reduction in sheet thickness. The optimized value for this coefficient was found to be 0.057 in the present research work.
- The gap between the matrix and the blank holder is of the other parameters affecting the hydro-mechanical deep drawing. With increasing this distance, the sheet edge has greater freedom for movement. In addition, due to the presence of fluid layer on the top and bottom of this region, wrinkling and reduced product uniformity are probable.

References

- [1] M. Koç, 2008, *Hydroforming for advanced manufacturing*, Elsevier,
- [2] S.-H. Zhang, J. Danckert, Development of hydro-mechanical deep drawing, *Journal of Materials Processing Technology*, Vol. 83, No. 1, pp. 14-25, 1998.
- [3] L. Lang, J. Danckert, K. B. Nielsen, Investigation into hydrodynamic deep drawing assisted by radial pressure: Part I. Experimental observations of the forming process of aluminum alloy, *Journal of Materials Processing Technology*, Vol. 148, No. 1, pp. 119-131, 2004.
- [4] R. A. Ayres, Alloying aluminum with magnesium for ductility at warm temperatures (25 to 250 C), *Metallurgical Transactions A*, Vol. 10, No. 7, pp. 849-854, 1979.
- [5] P. Groche, R. Huber, J. Dörr, D. Schmoeckel, Hydromechanical deep-drawing of aluminium-alloys at elevated temperatures, *CIRP Annals-Manufacturing Technology*, Vol. 51, No. 1, pp. 215-218, 2002.
- [6] K. Nakamura, Warm deep drawability with hydraulic counter pressure of 1050 aluminum sheets, *Japan Institute of Light Metals, Journal*, Vol. 47, No. 6, pp. 323-328, 1997.

- [7] H. Choi, M. Koç, J. Ni, A study on warm hydroforming of Al and Mg sheet materials: mechanism and proper temperature conditions, *Journal of Manufacturing Science and Engineering*, Vol. 130, No. 4, pp. 041007, 2008.
- [8] M. Hosseinpour, A. Gorji, M. Bakhshi, On the experimental and numerical study of formability of Aluminum sheet in warm hydroforming process, *Modares Mechanical Engineering*, Vol. 15, No. 2, 2015.
- [9] H. Gedikli, Ö. N. Cora, M. Koç, Comparative investigations on numerical modeling for warm hydroforming of AA5754-O aluminum sheet alloy, *Materials & Design*, Vol. 32, No. 5, pp. 2650-2662, 2011.
- [10] A. Hashemi, M. H. Gollo, S. H. SEYEDKASHI, Process window diagram of conical cups in hydrodynamic deep drawing assisted by radial pressure, *Transactions of Nonferrous Metals Society of China*, Vol. 25, No. 9, pp. 3064-3071, 2015.
- [11] R. K. Desu, S. K. Singh, A. K. Gupta, Comparative study of warm and hydromechanical deep drawing for low-carbon steel, *The International Journal of Advanced Manufacturing Technology*, Vol. 85, No. 1-4, pp. 661-672, 2016.
- [12] Q.-F. Chang, D.-Y. Li, Y.-H. Peng, X.-Q. Zeng, Experimental and numerical study of warm deep drawing of AZ31 magnesium alloy sheet, *International Journal of Machine Tools and Manufacture*, Vol. 47, No. 3, pp. 436-443, 2007.
- [13] S. Mahabunphachai, M. Koç, Investigations on forming of aluminum 5052 and 6061 sheet alloys at warm temperatures, *Materials & Design (1980-2015)*, Vol. 31, No. 5, pp. 2422-2434, 2010.
- [14] A. Ataee, E. Azarlu, Multi-objective Optimization of web profile of railway wheel using Bi-directional Evolutionary Structural Optimization, *Journal of Computational Applied Mechanics*, 2017.
- [15] J. H. Holland, 1992, *Adaptation in natural and artificial systems: an introductory analysis with applications to biology, control, and artificial intelligence*, MIT press,
- [16] M. Sharififar, S. Akbari Mousavi, Numerical study and genetic algorithm optimization of hot extrusion process to produce rectangular waveguides, *Journal of Computational Applied Mechanics*, Vol. 47, No. 2, pp. 129-136, 2016.
- [17] H. Mohammadi, M. Sharififar, A. A. Ataee, Numerical and Experimental Analysis and Optimization of Process Parameters of AA1050 Incremental Sheet Forming, *Journal of Computational Applied Mechanics*, Vol. 45, No. 1, pp. 35-45, 2014.
- [18] K. Deb, 2001, *Multi-objective optimization using evolutionary algorithms*, John Wiley & Sons,
- [19] Y. Aue-U-Lan, G. Ngaile, T. Altan, Optimizing tube hydroforming using process simulation and experimental verification, *Journal of Materials Processing Technology*, Vol. 146, No. 1, pp. 137-143, 2004.